Received: 3 October 2019 | Revised: 29 November 2019 | Accepted: 3 December 2019

DOI: 10.1002/qua.26142

FULL PAPER

International Journal of Quantum Chemistry WILEY

Ammonia, water, and hydrogen: Can nuclear motion be described classically?

Irmgard Frank | Stefanie Genuit | Florian Matz | Hedda Oschinski

Theoretische Chemie, Universität Hannover, Hannover, Germany

Correspondence
Irmgard Frank, Theoretische Chemie, Universität at Hannover, Callinstr. 3A, 30167 Hannover, Germany.
Email: irmgard.frank@theochem.uni-hannover.de

Abstract

The hypothesis that nuclear motion can be described classically has been tested for several critical systems. We investigate the inversion of ammonia and the heat capacities of water and hydrogen. We use conventional ab initio molecular dynamics, which describes nuclear motion classically and the electron cloud using density functional theory. Ammonia inversion is described perfectly by the tunneling of the p orbital through the molecular plane. Nuclear tunneling is not needed to describe this phenomenon. While the investigation of heat capacities is hampered by the brief simulation times and limited system sizes, we can nevertheless make some qualitative statements. Indeed, the heat capacity can be frozen out in molecular dynamics simulations of solids, and hence, a quantized description is not required.

KEYWORDS

chemical reactions, molecular dynamics

1 | INTRODUCTION

For almost 100 years, the Schrödinger equation[1] has been incredibly successful in describing any kind of matter. Most quantum mechanical calculations are performed for static problems using the time-independent Schrödinger equation for the electrons. This approach works perfectly for the quantum mechanical description of the electronic structure and allows us to describe molecular structure, electronic spectra, and many other phenomena. Currently, a classical description is usually used to describe the nuclear motion that controls chemical reactions.[2,3] While at first glance, this approach is used due to its simplicity, the classical description of nuclear motion also has several conceptual advantages compared to the full quantum mechanical treatment of molecular systems.[4,5]

In a complete quantum mechanical treatment, all objects do not have a well-defined position prior to measurement and we now know that this assumption is incorrect: First, experimentally, we now have a far better understanding of molecular systems compared to that at the time when quantum theory was first developed. Our more detailed knowledge about nanometer and sub-nanometer phenomena is due to the development of modern experimental techniques such as scanning tunneling microscopy. It is clear from such experiments with atomic resolution that for any molecular system, small nuclei are surrounded by an electron cloud. This electron cloud moves constantly as do the whole atoms. To some degree, the investigated system is influenced by the measurement, but this does not change the obtained results much in these highly sensitive experiments. The cloud never collapses.

Second, from a theoretical point of view, much can be learned from movies of chemical reactions that have been generated with ab initio molecular dynamics (AIMD), or more specifically Car-Parrinello molecular dynamics (CPMD).[2,3] In CPMD simulations, every molecular system, that is, any kind of matter, is treated as consisting of nuclei represented as points in space and of a surrounding electron cloud. We describe the molecular systems with differential equations and follow the development of the system over time. In an equilibration phase, the nuclear

velocities adopt a Maxwell-Boltzmann distribution because this is the most likely distribution. The electronic orbitals may become gradually more or less localized during a chemical reaction, but this occurs in a continuous motion. We have shown in many studies that chemical reactions can be described well using AIMD.

Finally, a simpler theory that does not lead to philosophical problems is generally preferable. We do not face philosophical problems in CPMD calculations, since every part of the investigated system moves deterministically at any time. When we determine both nuclear motion and the electron cloud using differential equations, we obtain a purely deterministic model. Since the nuclear positions move classically, tunneling is always electron tunneling. The different reaction pathways that may be observed in different simulation runs are explained by deterministic chaos.[6,7]

Let us go into more detail concerning this theory that allows us to simulate the motion of nuclei and electron clouds over time. In CPMD, the motion of the electrons is modeled using the quasi-classical Car-Parrinello equations. In a CPMD simulation run, first the electrons are optimized according to the Born-Oppenheimer potential energy surfaces using the density functional theory (DFT) approximation (or the Kohn-Sham approximation[8,9]). Then, the nuclei are moved according to Newton dynamics. This motion of the nuclei results in the deviation of the electrons from the Born-Oppenheimer surface as computed using the DFT approximation. This deviation is converted into a force acting on the molecular orbitals, which then oscillate back to the Born-Oppenheimer surface according to the CPMD equations. Hence, in a single time step, both the electrons and the nuclei are moved, albeit by different equations. This procedure can be repeated for several thousand steps. Since the time step must be chosen to be on the order of 0.1 fs, typical simulation times are on the order of picoseconds. The alternative AIMD method is Born-Oppenheimer molecular dynamics, in which the electronic orbitals are fully optimized for the potential energy surface for every time step. CPMD is more stable and less expensive than BOMD. For a related approach see also.[10]

We obtain a plausible and simple picture. The small nuclei and the extended electron cloud obey different differential equations, which is not surprising because they are different kinds of objects on the scale of our simulations. While the electronic wavefunction is an extended object and must be described by wave mechanics, the centers of the atoms move like particles. We do not consider relativistic effects, since nuclear motion at normal temperatures occurs on the scale of the velocity of sound, rather than on the scale of the velocity of light. If necessary, it would be easy to extend the theory to a relativistic treatment using special relativity for the nuclear motion. Additionally, we discuss processes at the nanometer scale only, that is, we do not describe phenomena connected to the inner structure of the nuclei, such as fission and fusion. This would demand a theory of the nuclear structure that would be able to explain the nuclide chart like the Schrödinger equation, together with the Pauli principle, explains the periodic system.

Many phenomena must be checked to confirm that nuclear motion can be accurately treated with a classical description. Some of these phenomena are treated in the present study. We use AIMD as a powerful but also limited tool for asking the question of whether a classical treatment is sufficient. The advantage of AIMD methods is that they ideally do not use information from experiments. Their disadvantage is the high amount of CPU time necessary to obtain converged results. AIMD can be applied to any kind of molecular system, that is, molecules, liquids, solutions, and solids. However, the high transferability of this method is contrasted with its limited numerical accuracy due to the use of the DFT approach for the electronic structure description.[8,9]

In the present study we have examined phenomena that have traditionally been considered to be proofs that all phenomena are described by the Schrödinger equation. The inversion of ammonia[11] is often (but not always[12]) viewed as a typical example of nuclear tunneling (see References [13–16] and literature cited therein). Another example of such phenomena are heat capacities, in particular those of the very light hydrogen molecule and of liquid water.[17]

2 | RESULTS AND DISCUSSION

2.1 | Ammonia: Inversion

The result for ammonia can be summarized in a few sentences as follows. The barrier is obtained correctly using standard density functionals (Becke-Lee-Yang-Parr, BLYP: 6.22 kcal/mol, B3LYP: 6.16 kcal/mol, exp.: 5.8 kcal/mol[18]). This barrier height determines the reaction velocity. It is problematic to consider the barrier width in order to describe nuclear tunneling. It is impossible to define such a barrier width rigorously for a multidimensional potential energy surface because unlike the barrier height, it does not correspond to a difference between state functions. If a reaction is slowed down by a "long" reaction pathway, it is better to take this phenomenon into account by an entropy contribution. This entropy contribution is small in the case of ammonia. There is no need for a special arrangement of the atoms for the reaction to occur. Once there is enough kinetic energy within the relevant degree of freedom, the isomerization typically occurs several times (Figure 1). In the first series of simulations, the molecule was fixed in space, that is, the rotational and translational degrees of freedom were set to zero (NH3.p.fix.mpg). The simulations show the tunneling of the p orbital through the molecular plane. The motion of the nuclei is described classically and merely follows the motion of the electronic wavefunction. Very similar results are obtained for deuterated ammonia (ND3.p.fix.mpg), but the reaction time is longer by ~36% on average (see Supporting information Video S1). Below 1000 K, we do not observe an inversion on the picosecond timescale for both NH_3 and ND_3.

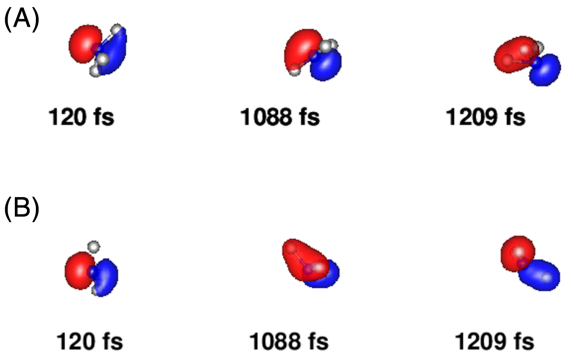

FIGURE 1 Ammonia inversion. The movies (see the Supporting Information) show the electron tunneling. A, The p orbital moves through the plane and the classically described nuclei follow (average temperature of the simulation run: 3700 K). B, Alternatively, if the molecule is allowed to rotate in space, a much more complex motion of the orbitals is observed (average temperature: 3400 K)[19]

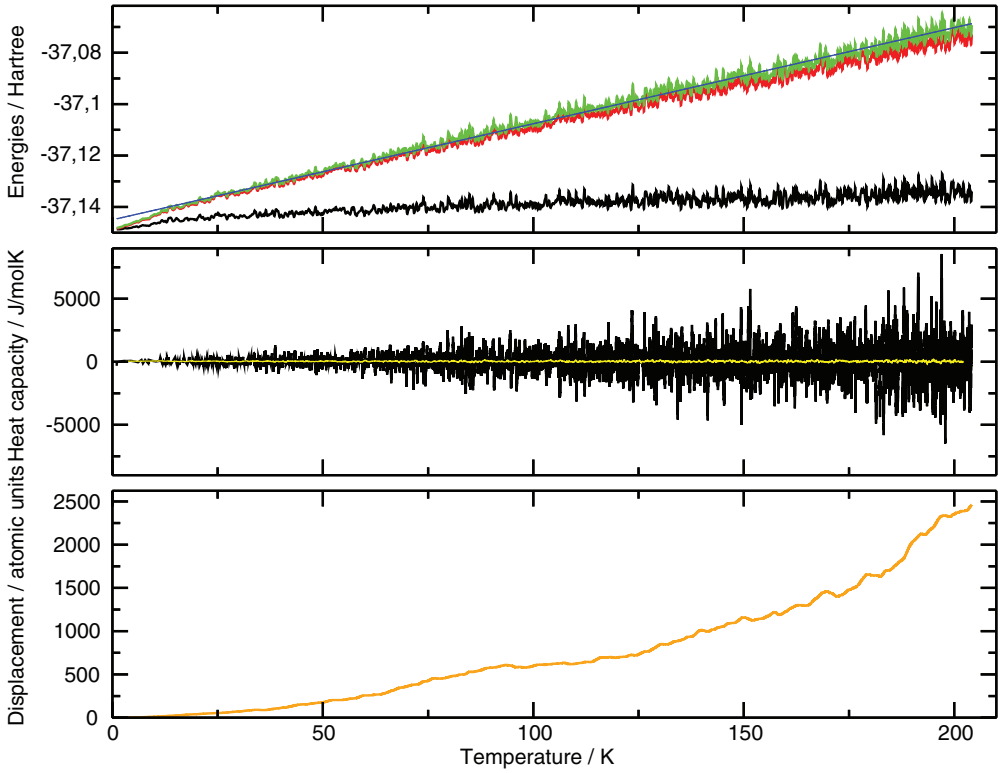

FIGURE 2 Example of the heating of hydrogen. Upper graph: total energy (green), classical energy (red) and Kohn-Sham energy (black); blue: linear regression. Middle graph: heat capacity $C_{V,m}$; yellow: average. Lower graph: mean square displacement of the nuclei. The results are plotted against the temperature with a heating rate of 0.001 kelvin/step. The linear regression of the total energy yields a value of the heat capacity of 30.66 J/(mol K); see the Supporting Information

The view changes if the molecules are allowed to rotate in space. Then, we observe what we called a tardy dance of molecular orbitals[19] (NH3.p.mpg and ND3.p.mpg). This motion is reminiscent of the Pauli principle, which states that a spin-1/2 particle must rotate two times before the original state is reached again. A similar rule appears to apply to single orbitals. The measurable total density is unaffected by this unitary molecular orbital rotation.

2.2 | Molecular hydrogen and water: Heat capacities

Heat capacities can be determined only qualitatively from an AIMD simulation. We can simulate the system for only a few picoseconds, that is, we heat the system within a few picoseconds from approximately zero kelvin to several thousand kelvin. Nevertheless, it is likely that the most important features are observed correctly. For these simulations, there is the question of whether translation can be frozen out in the classical description of the nuclei which assumes the absence of quantum effects. It is clear that the answer to this question is yes, and the comparison to the experimental results is not performed for a single atom or a few atoms in space but for a condensed phase sample that is either solid or liquid. This is evident from the movies of the molecular dynamics simulations. At low temperatures, trivial results wherein the nuclei hardly move are observed. The solid and the liquid phase are described qualitatively correctly both with classical molecular dynamics and with AIMD. This is also evident from the fact that properties such as the characteristic radial distribution function are described correctly using molecular dynamics.[3] In principle, it is possible to freeze out all degrees of freedom. There is nothing that makes a quantum treatment inevitable. Here, we utilize the classical Maxwell-Boltzmann distribution that emerges automatically during a molecular dynamics run because it is the most probable distribution.

To determine the heat capacity from an AIMD simulation, we heat the system linearly, that is, the temperature increases by the same amount in every time step, while the total energy is no longer constant. We then compute the derivative of the total energy with respect to the temperature (Figure 2). This cannot be considered to be a highly accurate approach because our heating rate is several orders of magnitude higher than the highest rate that can be realized experimentally.

Calculation	Temperature range/K	Heating rate/K/step	$C_{V,m}$/J/(mol K)
1	0-3200	0.01	43.42
1a	0-20	0.0001	48.28
1b	0-200	0.001	30.66
1c	0-1600	0.01	29.47

Notes: The first simulation 1 was performed using a smaller simulation cell.
Abbreviation: CPMD, Car-Parrinello molecular dynamics.

TABLE 1 Heat capacities of hydrogen as obtained with CPMD at different heating rates according to the linear regression of the total energy

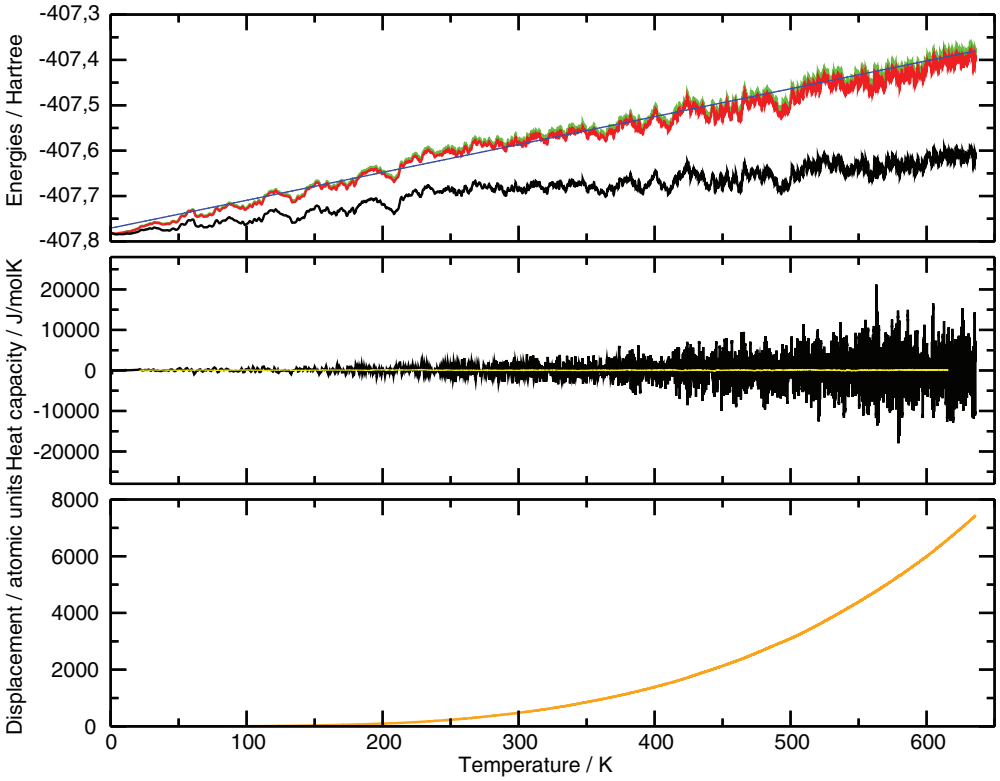

FIGURE 3 Example of the heating behavior of water. Upper graph: total energy (green), classical energy (red) and Kohn-Sham energy (black); blue: linear regression. Middle graph: heat capacity $C_{V,m}$; yellow: average. Lower graph: mean square displacement of the nuclei. The results are plotted against the temperature with a heating rate of 0.01 kelvin/step. The linear regression of the total energy yields a heat capacity value of 67.32 J/(mol K). For additional plots, see the Supporting Information

Calculation	Temperature range	Heating rate/K/step	$C_{V,m}$/J/(mol K)
2	200-900	0.1	75.27
2a	0-700	0.01	67.32
2b	0-80	0.001	78.55
2c	0-10	0.0001	83.15
2d	0-1000	0.1	72.15
2e	200-600	0.001	119.55
3	0-500	0.01	76.11
3a	20-450	0.01	103.15

Notes: In runs **3** and **3a** the simulation cell volume was increased by a factor of 2. For a more detailed evaluation of run **2e** see the Supporting Information, Figures S13 and S14.
Abbreviation: CPMD, Car-Parrinello molecular dynamics.

TABLE 2 Heat capacities of water and of hexagonal ice, respectively, as obtained by CPMD at different heating rates and temperature ranges using the linear regression of the total energy

We obtain a very noisy result due to the small number of particles considered in our simulations. Nevertheless, two clear conclusions can be drawn from these data: first, the heat capacity starts from small values (0-20 J/[mol K] within the error of the method), and second, it increases rapidly to meaningful high-temperature values (ideal gas: 3.5 R = 29.1 J/[mol K]); see Table 1.

Experimentally, the heat capacity $C_{p,m}$ of water is initially close to zero, and then increases more or less linearly until it jumps from about 37 J/(mol K) to higher values of ~75 J/(mol K) at ~270 K.[20,21] At about 370 K the value of the heat capacity jumps back to about 38 J/(mol K). In the simulations, we observe initial values close to zero. Additionally, the high-temperature value for $C_{V,m}$ is obtained in the right order of magnitude, see Figure 3 and Table 2. The ice structure slowly decomposes on the time scale of our simulations. An exception is run **2** in which the decomposition of the ice structure occurs right in the beginning. This does not change the picture provided by the results, with the exception of the presence of the strong uptake of energy in the beginning of this simulation run. The longest run, **2e** (450 000 steps), is evaluated in more detail in the Supporting Information (Figures S13 and S14). This evaluation shows that indeed at higher temperatures the heat capacity drops down again. For all shorter runs a linear regression for the complete run seemed to be the most meaningful procedure, showing that we get results in the right order of magnitude.

3 | CONCLUSIONS

In the present study, we successfully simulate the ammonia inversion from first principles using a code that describes nuclear motion classically. The barrier for the ammonia inversion is determined with quantitative accuracy as 6 kcal/mol. The simulations show electron tunneling through a wavefunction node while the hydrogen atoms follow this motion. However, the simulation times are not sufficiently long to serve as the basis of an Arrhenius plot. Once sufficient kinetic energy in the direction of the isomerization is available, several consecutive isomerization events are observed. The reaction velocity decreases when hydrogen is replaced by deuterium. The frequency of successful isomerizations at temperatures above 1000 K is on the order of magnitude of 2 THz and represents the upper limit for the room-temperature value. The frequency of the corresponding normally frustrated oscillation is found to be on the order of 200 THz. Our simulation times are far from sufficient for observing resonances close to the 1.27 cm line (0.03 THz) of ammonia used in masers.

While ammonia inversion can be simulated quite well using AIMD, the situation is less clear for the heat capacities. This is due to the limited system size and limited simulation time. The lack of clarity is likely not due to a more basic problem with the description of nuclear motion because some important features are described correctly. Furthermore, the error caused by the use of DFT should be of minor relevance because many properties such as the radial distribution functions are known to be obtained accurately with CPMD.[22–24]

Plotting the heat capacities against the temperature yields a very noisy result. However, the initial values of the curves are close to zero at zero kelvin. From the evaluation of several trajectories (see the Supporting Information), a marked deviation from zero to positive values is more often observed for hydrogen than for water, possibly because an amorphous sample rather than a perfect crystal was used for hydrogen. The high noise level precludes us from making more precise statements. The linear regression of the total energies vs temperature yields values for the high-temperature heat capacities in the correct order of magnitude. This is remarkable because this result was obtained solely from ab initio calculations without any use of experimental information. It appears that there is no need for a quantum mechanical description of nuclear motion. In principle, it can be frozen out completely in condensed phase experiments and simulations.

Furthermore, the successful use of CPMD shows that there is no reason to be reluctant to implement methods that use a second derivative with respect to time and hence describe space and time similarly. It is perfectly possible to describe the motion of the electron cloud on the basis of such a wave equation theory.

4 | METHODS

CPMD simulations[2,3,25] have been performed in the NVT ensemble (isochoric conditions) using the BLYP functional[26,27] together with the Grimme dispersion correction.[28] Troullier-Martins pseudopotentials optimized for the BLYP functional were employed for describing the core electrons.[29,30]

For the simulations of ammonia and a sample of 32 hydrogen molecules, the simulation cell was chosen as a cubic cell with the cell parameters of $8.5 \times 8.5 \times 8.5$ $Å^3$ ($16 \times 16 \times 16$ a.u.^{3}). Additional hydrogen calculations were carried out with a larger simulation cell ($10.6 \times 10.6 \times 10.6$ $Å^3$ ($20 \times 20 \times 20$ a.u.^{3}) to test the influence of pressure. The plane-wave cutoff that determines the size of the basis set, was set to 50.0 Rydberg. The time step was chosen as 5 a.u. (0.12 fs), and the fictitious electron mass was 400 a.u. The simulations were carried out at different temperatures for up to 400 000 steps, that is, for up to 48 ps.

For the simulations of water, we started with the hexagonal ice structure. An orthorhombic cutout of the ice structure was constructed with 24 molecules in the simulation cell (cell parameters: $13.5212 \times 7.8071 \times 7.3596$ $Å^3$ [$25.5513 \times 14.7533 \times 13.9076$ a.u.^{3}]). The same cutoff, time step, and electron mass were used. In additional calculations the volume of the cell was doubled to test the influence of pressure. Data were accumulated for up to 54 ps.

REFERENCES

[1] E. Schrödinger, *Ann. Physik* **1926**, *79*, 361.
[2] R. Car, M. Parrinello, *Phys. Rev. Lett.* **1985**, *55*, 2471.
[3] D. Marx, J. Hutter, *Ab Initio Molecular Dynamics: Basic Theory and Advanced Methods*, Cambridge University Press, Cambridge **2009**.
[4] I. Frank, *arXiv* **2014**, *1402*, 1133.
[5] I. Frank, *arXiv* **2016**, *1605*, 06954.
[6] C. Nonnenberg, I. Frank, T. Klapötke, *Angew. Chem. Int. Ed.* **2004**, *43*, 4586.
[7] F. Hofbauer, I. Frank, *Chem. Eur. J.* **2012**, *18*, 277.
[8] P. Hohenberg, W. Kohn, *Phys. Rev. B* **1964**, *136*, 864.
[9] W. Kohn, L. J. Sham, *Phys. Rev. A* **1965**, *140*, 1133.
[10] J. L. Alonso, X. Andrade, P. Echenique, F. Falceto, D. Prada-Gracia, A. Rubio, *Phys. Rev. Lett.* **2008**, *101*, 096403.
[11] C. E. Cleeton, N. H. Williams, *Phys. Rev.* **1934**, *45*, 234.
[12] C. Kölmel, C. Ochsenfeld, R. Ahlrichs, *Theor. Chem. Acta* **1991**, *82*, 271.
[13] S. T. Tserkis, C. C. Moustakidis, S. E. Massen, C. P. Panos, *Phys. Lett. A* **2014**, *378*, 497.
[14] C. Liu, J. Manz, Y. Yang, *J. Phys. B* **2015**, *48*, 164001.
[15] C. Liu, J. Manz, Y. Yang, *Phys. Chem. Chem. Phys.* **2016**, *18*, 5048.
[16] C. Fabri, R. Marquardt, A. G. Csaszar, M. Quack, *J. Chem. Phys.* **2019**, *150*, 014102.
[17] P. Atkins, J. de Paula, J. Keeler, *Atkins' Physical Chemistry*, 11th ed., Oxford University Press, Oxford **2018**, p. 560.
[18] A. Rauk, L. C. Allen, E. Clementi, *J. Chem. Phys.* **1970**, *52*, 4133.
[19] I. Frank, P. Kraus, *Int. J. Quantum. Chem.* **2018**, *118*, e25718.
[20] W. F. Giauque, J. W. Stout, *J. Am. Chem. Soc.* **1936**, *58*, 1144.
[21] R. C. Dougherty, L. N. Howard, *J. Chem. Phys.* **1998**, *109*, 7379.
[22] K. Laasonen, M. Sprik, M. Parrinello, R. Car, *J. Chem. Phys.* **1993**, *99*, 9080.
[23] E. S. Fois, M. Sprik, M. Parrinello, *Chem. Phys. Lett.* **1994**, *223*, 411.
[24] M. Sprik, J. Hutter, M. Parrinello, *J. Chem. Phys.* **1996**, *105*, 1142.
[25] CPMD, CPMD, Version 4.1, J. Hutter et al., http://www.cpmd.org/, Copyright IBM Corp 1990–2015, Copyright MPI für Festkörperforschung Stuttgart 1997–2001.
[26] A. Becke, *Phys. Rev. A* **1988**, *38*, 3098.
[27] C. Lee, W. Yang, R. G. Parr, *Phys. Rev. B* **1988**, *37*, 785.
[28] S. Grimme, *J. Comput. Chem.* **2006**, *27*, 1787.
[29] N. Troullier, J. L. Martins, *Phys. Rev.* **1991**, *43*, 1993.
[30] M. Boero, M. Parrinello, K. Terakura, H. Weiss, *Mol. Phys.* **2002**, *100*, 2935.

SUPPORTING INFORMATION

Additional supporting information may be found online in the Supporting Information section at the end of this article.

How to cite this article: Frank I, Genuit S, Matz F, Oschinski H. Ammonia, water, and hydrogen: Can nuclear motion be described classically? *Int J Quantum Chem*. 2020;120:e26142. https://doi.org/10.1002/qua.26142